

Experimental determination of BEDT-TTF⁺ electron-molecular vibration constants through optical microreflectance

G. Visentini and M. Masino

Dipartimento di Chimica Generale ed Inorganica, Chimica Analitica e Chimica Fisica, Università di Parma, I-43100 Parma, Italy

C. Bellitto

Istituto di Chimica dei Materiali, Consiglio Nazionale delle Ricerche, I-00016 Monterotondo Stazione 10, Roma, Italy

A. Girlando

Dipartimento di Chimica Generale ed Inorganica, Chimica Analitica e Chimica Fisica, Università di Parma, I-43100 Parma, Italy

(Received 12 January 1998; revised manuscript received 6 May 1998)

In the salt formed by bis(ethylenedithio)tetrathiafulvalene (BEDT-TTF) with the $[\text{Mo}_6\text{O}_{19}]^{2-}$ anion, the BEDT-TTF⁺ cations form quasi-isolated dimers. For this reason (BEDT-TTF)₂Mo₆O₁₉ has been selected to experimentally evaluate the BEDT-TTF⁺ microscopic parameters. Using the microreflectance technique we were able to collect polarized infrared/visible spectra from a single-crystal face. The analysis of the spectra in terms of the isolated dimer model yields reliable estimates of BEDT-TTF⁺ electron-molecular vibration (*e-mv*) coupling constants. The effective on-site electron-electron repulsion is also evaluated. A comparison is made with available theoretical estimates of *e-mv* coupling constants. The possible role of *e-mv* coupling in BEDT-TTF based superconductors is briefly discussed. [S0163-1829(98)01738-X]

I. INTRODUCTION

Bis(ethylenedithio)tetrathiafulvalene (BEDT-TTF) is at present the most important molecular structure in the field of organic superconductors.¹ Whereas there is no agreement on the mechanism of organic superconductivity, some experimental evidence points to a direct or indirect role of electron-phonon coupling.²⁻⁴ Since the proposal of a direct involvement of high-frequency *intramolecular* phonons,⁵ several *ab initio*⁶ and semiempirical^{7,8} calculations have been performed to assess the magnitude of the relevant microscopic parameters, the electron-molecular vibration (*e-mv*) coupling constants. For such large molecules as BEDT-TTF, however, the accuracy of the computational methods is limited, as shown for instance by the comparison between the results obtained through different numerical approaches.⁶⁻⁸ For other important molecules in the field of synthetic metals the spectroscopic determination of *e-mv* coupling constants has proved to be reliable and accurate, and has been generally preferred to the theoretical estimates.⁹⁻¹¹

The experimental determination of *e-mv* coupling constants is based on the analysis of the vibrational spectra, where typical features due to *e-mv* coupling are evident. The model generally adopted to analyze the data has been the dimer model originally developed by Rice.^{12,9} Dimerized stack structures are indeed often encountered in the quasi-one-dimensional crystals formed by electron acceptor/donor molecules such as TCNQ or TTF.⁹ At variance with these planar molecules, however, the nonplanar structure of BEDT-TTF, together with the large amplitude motion of the terminal-CH₂-units, acts against building good π overlap along a stacking axis. The presence of the extended orbitals of the BEDT-TTF sulfur atoms then causes increased inter-columnar interaction, and in most cases BEDT-TTF salts and

charge-transfer (CT) complexes show a pronounced two-dimensional character.¹ The bidimensionality is believed to be the origin of the peculiar properties of BEDT-TTF compounds, including superconductivity, but then the isolated dimer model^{9,12} cannot be reasonably applied to the typical BEDT-TTF structures to extract the *e-mv* coupling constants.¹³⁻¹⁵ For the above reasons, reliable experimental estimates of the BEDT-TTF *e-mv* coupling constants are not available.

Considering that *e-mv* coupling constants are molecular parameters, and as such *transferable* from one crystal to another,⁹ we have looked for BEDT-TTF salts suitable to the analysis in terms of the dimer model. The crystal of (BEDT-TTF)₂[Mo₆O₁₉] (Refs. 16,17) is a good candidate, since the structure consists of $[(\text{BEDT-TTF})_2]^{2+}$ dimers, arranged nearly perpendicularly one to another, and well separated by the bulky $[\text{Mo}_6\text{O}_{19}]^{2-}$ anions. In the present paper we report polarized microreflectance and powder Raman spectra of (BEDT-TTF)₂[Mo₆O₁₉]. From these data we obtain the first accurate experimental estimate of BEDT-TTF⁺ *e-mv* coupling constants. In addition, the analysis of the electronic part of the spectra also allows us to estimate the purely electronic parameters, namely the intradimer CT integral, *t*, and the effective on-site electron-electron repulsion, $U_{\text{eff}} = U - V$. The values of these parameters turn out to be in good agreement with the available theoretical¹⁸ and experimental^{19,20} estimates.

II. EXPERIMENTAL

BEDT-TTF and $[(\text{C}_2\text{H}_5)_4\text{N}]_2[\text{Mo}_6\text{O}_{19}]$ were prepared according to the methods described in the literature.^{21,22} They were both recrystallized twice from chloroform and acetonitrile, respectively, and the purity checked by elemental analyses. All solvents were reagent grade, freshly distilled

and deaerated prior to use. Few tenths mm wide black shiny platelets of $(\text{BEDT-TTF})_2[\text{Mo}_6\text{O}_{19}]$ (Ref. 17) were obtained by room-temperature electrocrystallization in a conventional H-shaped cell with platinum electrodes under argon atmosphere. Good quality crystals were obtained starting from a 1:1 $\text{CH}_3\text{CN}/1,1,2$ -trichloroethane solution of $[(\text{C}_2\text{H}_5)_4\text{N}]_2[\text{Mo}_6\text{O}_{19}]$ and BEDT-TTF. A constant current density of $1\text{--}3 \mu\text{A}/\text{cm}^2$ was maintained between the electrodes, separated by a glass frit. Crystals were harvested at the anode after three weeks.

Polarized normal incidence specular reflectance spectra in the $600\text{--}9000 \text{ cm}^{-1}$ region were taken from single crystals by a Bruker IFS66 FT spectrometer, with a KBr beamsplitter, and with globar and tungsten sources for the mid- and near-infrared (IR), respectively. The spectrometer was equipped with a Bruker A590 IR microscope (magnification factor 300, spot size $40 \mu\text{m}$, maximum incidence and collection angle 5°) and a liquid-nitrogen-cooled mercury-cadmium-telluride detector. The reflectance data were normalized to the reflectance of a high quality silver mirror. Much care has been taken in focusing the microscope on a smooth portion of the sample, so the measured spectra reproduce the *absolute* reflectance of the crystal. Nonabsolute polarized reflectance were measured in the range $11\ 000\text{--}18\ 000 \text{ cm}^{-1}$ by using a Quartz beamsplitter and by connecting the microscope to a Si detector through an optical fiber. In addition, the transmission of $(\text{BEDT-TTF})_2[\text{Mo}_6\text{O}_{19}]$ and $[(\text{C}_2\text{H}_5)_4\text{N}]_2[\text{Mo}_6\text{O}_{19}]$ powders were measured as nujol mulls between 400 and 4000 cm^{-1} . Room-temperature Raman spectra were obtained on microcrystalline powders diluted in KBr with a weight ratio of about 80:1, mildly pressed on a KBr disk. The Raman spectra were recorded with a multichannel triple spectrograph (Jobin-Yvon S3000) equipped with a CCD detector. The Ar^+ laser (Coherent) line at 488.0 nm (about 15 mW) was focused by a cylindrical lens to a slitlike image $150 \mu\text{m}$ wide.

III. RESULTS

We have collected several polarized reflectance spectra of $(\text{BEDT-TTF})_2[\text{Mo}_6\text{O}_{19}]$ crystals, varying the angle between the polarization direction and the crystal axes, and using different samples. Two low-energy electronic bands are always present around 4500 and 7000 cm^{-1} . A polarization has been found that greatly enhances the relative intensity of the higher frequency band. In the polarization perpendicular to the above the lower frequency band reaches the maximum of intensity with respect to the other, even if both remain present in the spectrum. In the following, we will refer to the two directions of polarization as \parallel and \perp , respectively. The reflectance spectra corresponding to the two extreme polarizations are reported in Fig. 1. In the figure we observe a third absorption around $12\ 000 \text{ cm}^{-1}$, with highest intensity in the \parallel polarization. We attribute this band to the next-highest occupied molecular orbital (HOMO) to HOMO intramolecular (excitonic) transition of BEDT-TTF⁺.²⁴ Notice that due to the change of beamsplitter and detector, the reflectance beyond $10\ 000 \text{ cm}^{-1}$ does not connect well to the lower frequency data, and the corresponding reflectance values cannot be considered as absolute.

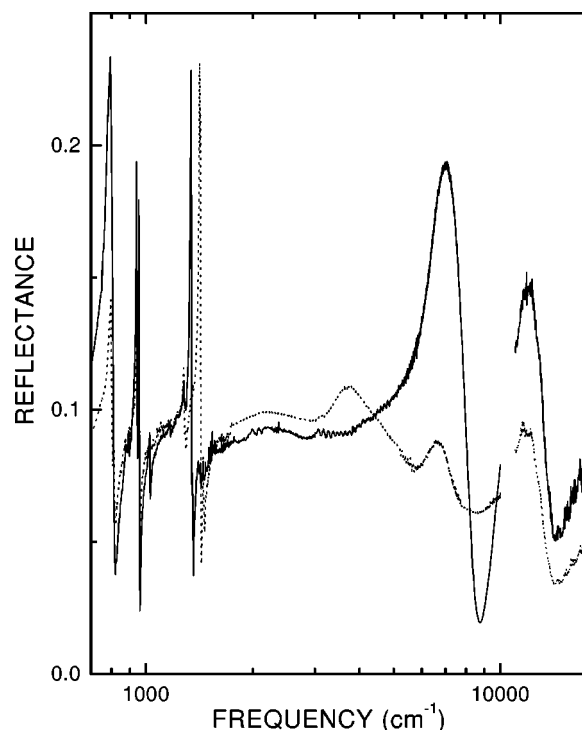


FIG. 1. Reflectance spectra of $(\text{BEDT-TTF})_2[\text{Mo}_6\text{O}_{19}]$ between 700 and $18\ 000 \text{ cm}^{-1}$. Note the logarithmic frequency scale. The solid and dotted lines correspond to \parallel and \perp polarization, respectively (see text).

A Kramers-Kronig transformation has been performed in the range $600\text{--}9000 \text{ cm}^{-1}$ by extrapolating the reflectance data to zero frequency with a constant value equal to that measured at the lowest frequency, as appropriate for a semiconductor. In extrapolating the data to high frequencies we have simulated the presence of the observed intramolecular, excitonic band of BEDT-TTF⁺ at $12\ 000 \text{ cm}^{-1}$ and followed standard procedures²⁵ for higher frequencies. Such kind of extrapolation is expected to influence the conductivity spectra only near the upper-frequency limit of the measured spectra. The conductivity spectra corresponding to the two extreme polarizations are reported in Fig. 2(a).

The strong electronic band at 7000 cm^{-1} is easily associated to the intradimer CT transition, so that the \parallel polarization, that sharply maximizes this band, corresponds to a direction perpendicular to the BEDT-TTF molecular planes. To identify the \perp direction of polarization, and assign the 4500 cm^{-1} band, we have calculated by the extended Hückel theory (EHT) all interdimer CT integrals within a radius of 10 \AA . The CT integral for any pair of BEDT-TTF molecules has been evaluated from the splitting of the frontier orbitals.^{23,18} We find $t_{\parallel} = 0.25 \text{ eV}$, whereas the only other non-negligible CT integral corresponds to the interaction between dimers in neighboring unit cells, translated along the a axis. We assume that this direction corresponds with the \perp polarization, assigning the 4500 cm^{-1} band to a lateral CT transition between dimers.²⁴

An enlarged portion of the conductivity spectrum in the region of molecular vibrations is reported in Fig. 3(a). For the $400\text{--}600 \text{ cm}^{-1}$ region, where no microreflectance data are available, we report the (unpolarized) absorption spectrum on nujol mulls. As it is well known,²⁶ for very thin

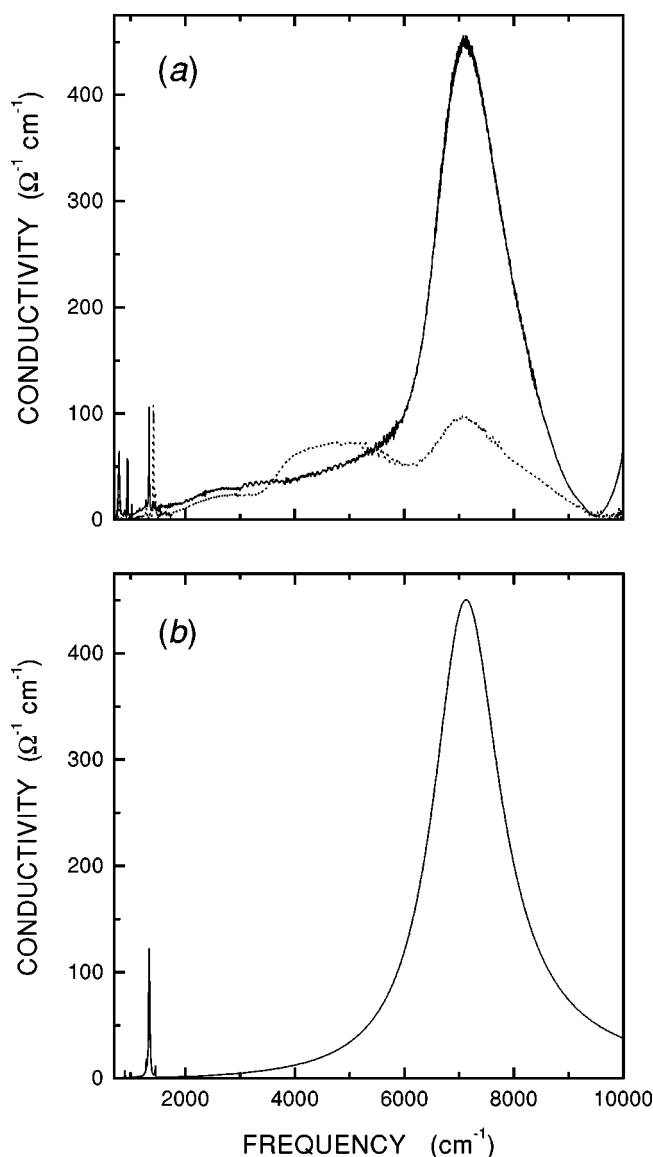


FIG. 2. Conductivity spectra of $(\text{BEDT-TTF})_2[\text{Mo}_6\text{O}_{19}]$ between 700 and 10 000 cm^{-1} . (a) Experimental spectrum for \parallel (solid line) and \perp (dotted line) polarizations; (b) \parallel spectrum calculated according to the isolated dimer model.

samples the IR absorption spectra can be considered proportional to the conductivity spectra. The intensities are normalized to the 1343 cm^{-1} vibronic band of the \parallel conductivity spectrum. In the \parallel spectra of Fig. 3(a) the bands corresponding to the main Raman bands (shown schematically as lines in the figure) are recognized as due to the e - mv coupling,^{12,10,11} and are the basis for the assessment of the e - mv coupling strength. The room-temperature Raman spectrum is reported in Fig. 4, and the observed IR and Raman frequencies are reported in Table I.

From a comparison with the spectra of $[(\text{C}_2\text{H}_5)_4\text{N}]_2[\text{Mo}_6\text{O}_{19}]$ we can easily identify the IR and Raman²⁷ bands due to the anion, as reported in the last column of Table I and marked in Fig. 3(a) by an asterisk. In order to facilitate the comparison with previous work,^{6-8,30} we follow Kozlov *et al.*⁷ in adopting a D_{2h} molecular symmetry for the classification of the normal modes. BEDT-TTF^+ is not planar, and has a lower molecular sym-

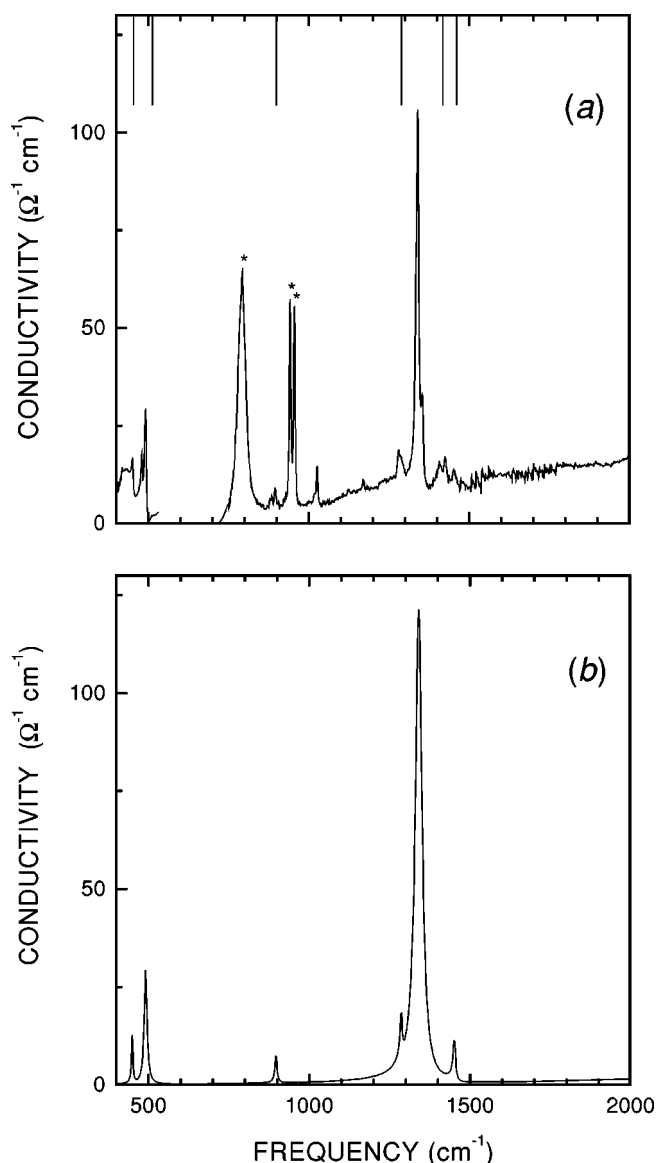


FIG. 3. (a) Single-crystal conductivity spectrum of $(\text{BEDT-TTF})_2[\text{Mo}_6\text{O}_{19}]$ between 700 and 2000 cm^{-1} (\parallel polarization) and powders absorption spectrum between 400 and 600 cm^{-1} . The Raman frequencies assigned to a_g modes are shown as vertical lines, whereas the IR bands due to the anion are marked by an asterisk; (b) e - mv induced spectrum calculated according to the isolated dimer model.

metry (D_2), which is also different from that of the neutral molecule (C_2).^{28,29} On the other hand, correlations between the spectral predictions based on D_{2h} and on D_2 symmetry are easily made, the difference being associated with the lack of inversion center (a_g and a_u become a , b_{1g} and b_{1u} become b_1 and so on). Moreover, the molecular vibrations most likely coupled to the electrons are those of the central tetrathiafulvalene (TTF) skeleton, so the use of the full symmetry of central unit allows a simpler analysis and a direct comparison with other TTF-based molecules.

The Raman and IR spectra of $(\text{BEDT-TTF})_2[\text{Mo}_6\text{O}_{19}]$ are interpreted on the basis of the present polarized IR data, with the help of the available assignments of BEDT-TTF^+ .⁷ In the present paper we are interested in the effects of the e - mv coupling, not in the details of the vibrational assign-

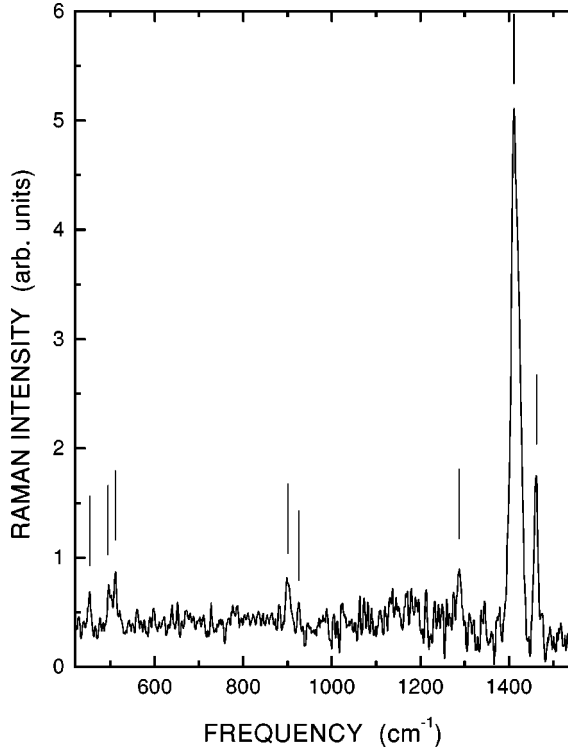


FIG. 4. Room-temperature Raman spectrum of (BEDT-TTF)₂[Mo₆O₁₉] powders diluted in KBr. Exciting line: 488.0 nm. The bands listed in Table I are put in evidence by a short vertical line.

ments. Therefore we shall limit the discussion to the identification of the totally symmetric modes, avoiding comments on the weakest bands, whose origin is doubtful (nontotally symmetric modes, combinations and overtones, etc.). The Raman bands due to totally symmetric modes, and the corresponding bands activated in IR by the coupling to the electrons,⁹ are rather easily identified. The assignment is reported in the last column of Table I. The assignment of $a_g \nu_7$ and ν_{10} modes to the Raman bands at 899 and 453 cm⁻¹ (with IR vibronic counterparts at 897 and 450 cm⁻¹, respectively), appears to be different from previous proposals on other BEDT-TTF salts,^{7,31,32} but it is induced by the analysis of the e - mv coupling. A comment is deferred to after such analysis has been made.

We can now calculate the frequency-dependent conductivity in the \parallel direction within the isolated dimer approximation. Following Rice,¹² for the electronic part we consider only the ground and CT state, disregarding the presence of excitonic (intramolecular) excited states. Furthermore, the coupling between electrons and the molecular vibrations is assumed to occur through the phononic modulation of the on-site energy. Thus, only the normal modes totally symmetric in the molecular symmetry are coupled to the electrons.¹⁰ The corresponding microscopic parameters are the linear e - mv coupling constants, defined as $g_j = (\partial\epsilon/\partial Q_j)$, where ϵ is the on-site energy and Q_j the j th dimensionless normal coordinate. Using linear-response theory, the frequency-dependent conductivity in the direction of the CT transition is given by¹² ($\hbar = 1$):

$$\sigma(\omega) = -i\omega \frac{e^2 a^2}{4} N_d \frac{\chi(\omega)}{1 - \tilde{\chi}(\omega)D(\omega)}, \quad (3.1)$$

where e is the electronic charge, a is the intradimer distance, N_d is the number of dimers per unit volume, $\chi(\omega) = 2|\mu_{CT}|^2 \omega_{CT} / (\omega_{CT}^2 - \omega^2 - i\omega\gamma_{CT})$ is the CT electronic susceptibility, and $\tilde{\chi}(\omega) = \chi(\omega)/\chi(0)$ its reduced form. The e - mv coupled phonons are described in the phonon propagator:

$$D(\omega) = \chi(0) \sum_j \frac{g_j^2}{\omega_{0,j}^2 - \omega^2 - i\omega\gamma_j}, \quad (3.2)$$

where $\omega_{0,j}$ and γ_j are the frequencies and damping factors of the unperturbed (uncoupled) phonons.

Expression (3.1) for $\sigma(\omega)$ describes the electronic CT absorption and a series of IR bands corresponding to the e - mv coupled modes, which borrow intensity from the electronic transition. These modes correspond to the antiphase combinations of the totally symmetric vibrations of the individual modes, whereas the in-phase combinations (active in Raman) are completely decoupled from the electronic system. In order to obtain the dimer microscopic parameters one can fit $\text{Re}[\sigma(\omega)]$ to the experimental spectrum. However, in such nonlinear fitting the final values of the parameters, in particular of the g 's, are to some extent bound to the initial choices. Furthermore, quite often the unperturbed frequencies have been considered themselves as adjustable parameters, or have been derived from the IR data,¹⁵ adding a source of uncertainty to the final fitting parameters.

Years ago we suggested⁹ a more direct procedure to evaluate the e - mv coupling constants, without nonlinear fittings and relying completely on the experimental data. The poles of the phonon propagator (3.2) correspond to the frequencies Ω_j of the observed e - mv induced bands, whereas the $\omega_{0,j}$ are given directly by the Raman spectrum (Table I). The unknown g 's are then calculated by solving a set of linear equations, that in simplified form can be written as

$$\chi(0) \sum_k g_k^2 \prod_{l \neq k} (\omega_{0,l}^2 - \Omega_j^2) = \prod_l (\omega_{0,l}^2 - \Omega_j^2), \quad (3.3)$$

where $\chi(0)$ is evaluated from the frequencies and oscillator strength of the CT transition and from the known a and N_d . The resulting BEDT-TTF⁺ e - mv coupling constants are reported in Table II. The conductivity spectrum is then calculated from Eq. (3.1), the unperturbed damping factors being the only adjustable parameters.

The good agreement between experimental and calculated conductivity in the vibrational spectral region [Figs. 3(a) and 3(b), respectively] provides an *a posteriori* test of the accuracy of the estimated coupling constants. They have been derived only by using Table I Raman and IR frequencies, so that the striking agreement between calculated and experimental intensities offers a nice confirmation of the validity of the adopted model and of the vibrational assignments. In particular, we remark that the relative intensities of the e - mv induced bands in the 350–450 cm⁻¹ spectral region are properly reproduced only by assigning the $a_g \nu_{10}$ to the 453 cm⁻¹ Raman band rather than to the 496 cm⁻¹ one.^{7,32} The assignment of the Raman band at 899 cm⁻¹ requires more extensive comments. In the case of some BEDT-TTF^{0.5+} salts a Raman band around 890 cm⁻¹ (with IR counterpart shifted by about 10 cm⁻¹) was assigned to

TABLE I. Infrared and Raman frequencies (400–1600 cm^{-1}) of (BEDT-TTF) $_2$ [Mo $_6$ O $_{19}$].

$\bar{\nu}/\text{cm}^{-1}$	Raman Rel. Int. ^b	$\bar{\nu}/\text{cm}^{-1}$	Infrared Rel. Int. ^b	Pol.	Assignments ^a		
453	mw	450	mw		$a_g \nu_{10}$		
		479	m		b_{1u} or b_{3u}		
496	mw				b_{1g} or b_{2g}		
513	m	491	ms		$a_g \nu_9$		
		793	vs		} $[\text{Mo}_6\text{O}_{19}]^{2-}$		
		797	ms	\perp			
		814	m	\perp			
		884	vw				
899	mw	897	mw		$b_{3g} \nu_{60}?$		
		902	vw	\perp	$a_g \nu_7$		
925	vw				a_u, b_{3g} or b_{3u}		
		942	vs	, \perp	$[\text{Mo}_6\text{O}_{19}]^{2-}$		
		957	vs	, \perp	$[\text{Mo}_6\text{O}_{19}]^{2-}$		
		1027	mw (vw)	(\perp)	$b_{1u} \nu_{30}$ or $b_{2u} \nu_{47}$		
		1170	vw				
1288	vw	1280	m (sh)	\perp ()	$b_{1u} \nu_{29}$		
		1284	m		$a_g \nu_5$		
		1294	w	\perp			
1414	vs	1343	vs		} $a_g \nu_3$		
1418	sh	1356	sh				
1460	s				$b_{2u} \nu_{45}$		
				1408	w (sh)	(\perp)	$b_{1u} \nu_{28}$
				1419	vs	\perp	
				1422	vs	\perp	
				1426	w		
				1452	w		$a_g \nu_2$
		1454	mw	\perp	$b_{1u} \nu_{27}$		

^aClassification following assumed D_{2h} molecular symmetry. The mode numbering is from Ref. 30.

^bQualitative relative intensities expressed as: vs, very strong; s, strong; ms, medium strong; m, medium; mw, medium weak; w, weak; vw, very weak; sh, shoulder.

TABLE II. Electron-molecular vibration ($e-mv$) coupling constants, g_i , and small polaron binding energy of BEDT-TTF $^+$ radical cation.

Mode	Frequency (cm^{-1})		Present work	g_i (meV)	
	Obs.	Calc.		Calc., MNDO ^a	Calc., <i>ab initio</i> ^b
$a_g \nu_1$		2912		8	15
ν_2	1460	1465	43	30	107
ν_3	1414	1427	71	132	51
ν_4		1421	~ 0	18	14
ν_5	1288	1287	6	10	8
ν_6		979	~ 0	17	10
ν_7	899	896	12	13	15
ν_8		672	~ 0	16	12
ν_9	513	508	40	30	22
ν_{10}	453	483	12	3	4
ν_{11}		318		~ 0	2
ν_{12}		159		~ 0	~ 0
E_{SP} (meV)			68	127	90

^aReference 7.

^bReference 6.

the $b_{3g} \nu_{60}$ on the basis of the calculated isotopic frequency shifts of the neutral molecule.^{30,31} However, there is nothing unique about calculated isotopic frequency shifts for single modes, and indeed more recent *ab initio* calculations report different shifts:³³ on their basis, also the assignment to the $b_{3g} \nu_{60}$ mode would be excluded. As a matter of fact, many different modes are predicted to occur in the 900–1000 cm^{-1} spectral region. A safe and definite assignment is then a very difficult task, also complicated by the change of molecular symmetry from the neutral to ionized BEDT-TTF. On the other hand, Fig. 3 shows that for (BEDT-TTF)₂[Mo₆O₁₉] the intensity of the IR counterpart of the Raman band at 899 cm^{-1} is properly reproduced by our calculated *e-mv* induced spectrum. This fact suggests that the involved mode modulates the on-site energy and is therefore totally symmetric (a under D_2 , a_g or a_u under D_{2h}). In the lack of an unquestionable proof of the contrary, we therefore choose to assign the Raman band at 899 cm^{-1} to the $a_g \nu_7$ mode.

From the frequency and intensity of the CT transition we can also extract the values of the charge-transfer integral and the effective Hubbard U_{eff} . We find $t_{\parallel} = 0.3$ eV and $U_{\text{eff},\parallel} = 0.46$ eV. The measured t is in good agreement with the EHT value (see above) and with the *ab initio* transfer integral calculated on κ -phase BEDT-TTF salts,¹⁸ where similar dimeric structures are recognized. At the same time, our U_{eff} compares favorably with experimental estimates for κ phases, ranging from 0.4 to 0.7 eV,^{19,20} and with *ab initio* estimates¹⁸ yielding $U - V = 0.5$ eV. A comparison of the experimental [Fig. 2(a)] and calculated electronic \parallel spectra [Fig. 2(b)] shows good agreement, with some discrepancy around 4000 cm^{-1} , where a residual of the lateral CT transition alters the baseline.

IV. DISCUSSION AND CONCLUSIONS

Before commenting on Table II, it is worth to analyze the various sources of error and the approximations made in the determination of BEDT-TTF⁺ *e-mv* coupling constants. The microreflectance technique allowed us to use a single-crystal face, so that we get a fairly accurate measure of absolute reflectance, particularly if compared to measurements made on crystal mosaics. Unfortunately, due to limitations in our experimental apparatus, absolute reflectance measurements are only possible below 9000 cm^{-1} . Rather than arbitrarily connect the absolute and nonabsolute reflectance spectra below and above 9000 cm^{-1} , we have performed the Kramers-Kronig analysis only on the lower part of the spectra, simulating in the high-frequency extrapolation the presence of the observed excitonic band of BEDT-TTF⁺ at 12 000 cm^{-1} . We checked that the conductivity spectrum in the region of interest shows little dependence on the extrapolation procedure.

The spectrum has been analyzed in terms of the isolated dimer model,¹² which applies well to (BEDT-TTF)₂[Mo₆O₁₉], where quasi-isolated BEDT-TTF⁺ dimers are found. The presence of the nearby excitonic transition has not been taken into account. On the other hand, the above simplification has always been adopted in the previous spectroscopic determination of *e-mv* coupling constants,^{10,11} which also used the isolated dimer model to simulate a

dimerized stack. In the present case we have also observed a lateral CT transition around 4500 cm^{-1} , but since its dipole moment is almost perpendicular to that of the intradimer CT transition, the interaction between the two is expected to be small. As a check, we have also independently analyzed the \perp electronic spectrum in terms of the dimer model. The resulting electronic parameters are: $t_{\perp} = 0.06$ eV and $U_{\text{eff},\perp} = 0.56$ eV. The t_{\perp} value is similar to the calculated value from EHT, and the value of $U_{\text{eff},\perp}$ is not very different from the measured value in the \parallel direction. The vibronic part of the \perp conductivity has been also calculated in the isolated dimer approximation.¹² The calculated IR vibronic bands are very weak, so that they could hardly be identified in the spectra.

We now turn to the comparison of our experimental *e-mv* coupling constants with those calculated by semiempirical [modified neglect of differential overlap (MNDO)]⁷ and *ab initio*⁶ methods, also reported in Table II. The comparison is limited to the calculations performed for the BEDT-TTF cation, since it is known that the g 's values may change with the average charge of the molecule, due to normal mode mixing and/or to second-order *e-mv* coupling.⁹ In all estimates the most strongly coupled modes are the $a_g \nu_2$, ν_3 , and ν_9 . The ν_2 and ν_3 vibrations are very close in frequency, so it is difficult to precisely calculate the corresponding normal coordinates. This causes large differences in the calculated ratio g_2/g_3 . Our experimental estimate gives a clear indication, helping to settle the matter.

The energy gain due to the relaxation of the lattice consequent to the addition or removal of one electron, namely, the small polaron binding energy, $E_{\text{SP}} = \sum_i (g_i^2 / \omega_{0,i})$, is a measure of the overall electron-phonon interaction energy. We find $E_{\text{SP}} = 68$ meV, to be compared (bottom of Table II) with the MNDO and *ab initio* values of 127 and 90 meV, respectively. The agreement with *ab initio* calculation is reasonable, considering that the computed values are generally somewhat overestimated,¹¹ and that many very weakly coupled phonons contribute in the calculation. These small numbers are possibly within the uncertainties of theoretical estimates, and in any case are not experimentally accessible, since the corresponding *e-mv* induced bands have a too small intensity.

As in the other TTF-based electron acceptor molecules, three phonons largely dominate the BEDT-TTF⁺ overall *e-mv* coupling strength. These are the already mentioned $a_g \nu_2$, ν_3 , and ν_9 modes, described as two C=C stretching and a ring breathing, respectively. Indeed, these vibrations account for over 90% of the small polaron binding energy. It is instructive then to compare the present experimental estimate of the *e-mv* coupling strength of these three modes with the corresponding estimates available for other TTF-based molecules, namely TTF itself,⁹ tetramethyl-tetrathiafulvalene (TMTTF),³⁴ and dibenzo-tetrathiafulvalene (DBTTF).¹⁰ Table III reports the relevant *e-mv* coupling constants, together with the contribution to the small polaron binding energy, E_{SP} . It is seen that in both TTF and TMTTF the strength of *e-mv* interaction is significantly larger than in DBTTF or BEDT-TTF. This finding may be explained in terms of a larger delocalization of the HOMO in the latter molecular structures. The strength of *e-mv* coupling does not appear to be correlated to the superconducting properties,

TABLE III. Electron–molecular vibration (e - mv) coupling constants, g_i , and small polaron binding energy of the most relevant modes, for several TTF derivatives radical cations.

Mode	TTF ^a		TMTTF ^b		DBTTF ^c		BEDT-TTF ^d	
	Freq. (cm ⁻¹)	g_i (meV)	Freq.	g_i	Freq.	g_i	Freq.	g_i
a_g ν_2	1505	42	1567	32	1555	19	1460	43
ν_3	1420	133	1418	133	1409	79	1414	71
ν_9	501	71	523	56	512	53	513	40
E_{SP} (meV)		191		154		82		64

^aReference 9.

^bAdapted from Ref. 34.

^cReference 10.

^dPresent work.

since among the above donors only BEDT-TTF and an omologue of TMTTF, tetramethyl-tetraselenofulvalene (TMTSF) give superconducting salts. Of course many other factors, such as the degree of bidimensionality, the strength of electron-electron interaction and so on, are important or essential to organic superconductivity. The above comparison only suggests that the *intramolecular* vibrations are not *directly* involved in the superconductivity mechanism. On the other hand, indirect involvement, for instance through a polaron narrowing mechanism,³⁵ is in any case still possible. From this point of view, the present study, assessing the strength of e - mv coupling in BEDT-TTF structure, offers an important reference point in investigations on organic superconductivity. Moreover, the knowledge of the individual e - mv coupling constants is of help in the interpretation of the complex optical spectra of conducting and superconduct-

ing BEDT-TTF salts. For instance, a preliminary analysis shows that the Raman-IR frequency shifts observed for a_g modes of BEDT-TTF superconducting salts³¹ can be satisfactorily accounted for by our e - mv coupling constants together with a proper estimate³⁶ of the relevant $\chi(0)$ in Eq. (3.3).

ACKNOWLEDGMENTS

This work has been supported by the Ministry of University and Scientific and Technological Research (M.U.R.S.T.) and by the National Research Council (C.N.R.) of Italy. We gratefully thank Professor R. Bozio (Padova University) for allowing us to measure the Raman spectra in his laboratory, and M. Zanetti for technical support. We also acknowledge helpful discussions with Dr. A. Painelli.

¹J. M. Williams, A. J. Schultz, U. Geiser, K. D. Carlson, A. M. Kini, H. H. Wang, W.-K. Kwok, M.-H. Whangbo, and J. E. Shirber, *Science* **252**, 1501 (1991); J.M. Williams, J.R. Ferraro, R.J. Thorn, K.D. Carlson, U. Geiser, H.H. Wang, A.M. Kini, and M.-H. Whangbo, *Organic Superconductors (including Fullerenes)* (Prentice Hall, Englewood Cliffs, NJ, 1992).

²T. Ishiguro and K. Yamaji, *Organic Superconductors* (Springer-Verlag, Berlin, 1989).

³V. Merzhanov, P. Auban-Senzier, C. Bourbonnais, D. Jérôme, P. Batail, J.-P. Buisson, and S. Lefrant, *C. R. Acad. Sci., Ser. I: Math.* **314**, 563 (1992).

⁴A. M. Kini, K. D. Carlson, H. H. Wang, J. A. Schlueter, J. D. Dudek, S. A. Sirchio, U. Geiser, K. R. Lykke, and J. M. Williams, *Physica C* **264**, 81 (1996), and references therein.

⁵K. Yamaji, *Solid State Commun.* **61**, 413 (1987).

⁶J. C. R. Faulhaber, D. Y. K. Ko, and P. Briddon, *Synth. Met.* **60**, 227 (1993).

⁷M. E. Kozlov, K. I. Pokhodnia, and A. A. Yurchenko, *Spectrochim. Acta A* **45**, 437 (1989).

⁸J. Shumway, S. Chattopadhyay, and S. Satpathy, *Phys. Rev. B* **53**, 6677 (1996).

⁹A. Painelli, A. Girlando, and C. Pecile, *Solid State Commun.* **52**, 801 (1984); A. Painelli and A. Girlando, *J. Chem. Phys.* **84**, 5655 (1986).

¹⁰C. Pecile, A. Painelli, and A. Girlando, *Mol. Cryst. Liq. Cryst.*

171, 69 (1989), and references therein.

¹¹R. Bozio and C. Pecile, *Charge Transfer Crystals and Molecular Conductors (Spectroscopy of Advanced Materials)*, edited by R. J. H. Clark and R. E. Hester (Wiley, Chichester, 1991), and references therein.

¹²M. J. Rice, *Solid State Commun.* **31**, 93 (1979).

¹³T. Sugano, H. Hayashi, M. Kinoshita, and K. Nishikida, *Phys. Rev. B* **39**, 11 387 (1989).

¹⁴M. E. Kozlov, V. Ivanov, and K. Yakushi, *J. Phys.: Condens. Matter* **8**, 1011 (1996).

¹⁵H.-L. Liu *et al.*, *Chem. Mater.* **9**, 1865 (1997).

¹⁶S. Triki, L. Ouahab, and D. Grandjean, *Acta Crystallogr., Sect. C: Cryst. Struct. Commun.* **47**, 645 (1991).

¹⁷D. Attanasio, C. Bellitto, M. Bonamico, V. Fares, and S. Patrizio, *Synth. Met.* **41-43**, 2289 (1991).

¹⁸A. Fortunelli and A. Painelli, *Phys. Rev. B* **55**, 16 088 (1997).

¹⁹H. Mayaffre, P. Wzietek, D. Jérôme, C. Lenoir, and P. Batail, *Europhys. Lett.* **28**, 205 (1994).

²⁰J. Caulfield, W. Lubczynski, F. L. Pratt, J. Singleton, D. Y. K. Ko, W. Hayes, M. Kurmoo, and P. Day, *J. Phys.: Condens. Matter* **6**, 2911 (1994).

²¹J. Larsen and C. Lenoir, *Synthesis* **2**, 134 (1989).

²²M. Che, M. Fournier, and J. P. Launay, *J. Chem. Phys.* **71**, 1954 (1979).

²³P. M. Grant, *Phys. Rev. B* **26**, 6888 (1982).

- ²⁴T. Hasegawa, S. Kagoshima, T. Mochida, S. Sugiura, and Y. Iwasa, *Solid State Commun.* **103**, 489 (1997).
- ²⁵F. Wooten, *Optical Properties of Solids* (Academic, New York, 1972).
- ²⁶J. C. Decius and R. M. Hexter, *Molecular Vibrations in Crystals* (McGraw-Hill, New York, 1977), p. 190.
- ²⁷D. Pedron, A. Speghini, V. Mulloni, and R. Bozio, *J. Chem. Phys.* **103**, 2795 (1995).
- ²⁸E. Demiralp, S. Dasgupta, and W. A. Goddard III, *J. Am. Chem. Soc.* **117**, 8154 (1995).
- ²⁹R. Liu, X. Zhou, and H. Kasmai, *Spectrochim. Acta A* **53**, 1241 (1997).
- ³⁰J. E. Eldridge, C. C. Homes, J. M. Williams, A. M. Kini, and H. H. Wang, *Spectrochim. Acta A* **51**, 947 (1995).
- ³¹J. E. Eldridge, Y. Xie, H. H. Wang, J. M. Williams, A. M. Kini, and J. A. Schlueter, *Spectrochim. Acta A* **52**, 45 (1996); J.E. Eldridge, Y. Xie, Y. Lin, C.C. Homes, H.H. Wang, J.M. Williams, A.M. Kini, and J.A. Schlueter, *ibid.* **53**, 565 (1997).
- ³²H. H. Wang, A. M. Kini, and J. M. Williams, *Mol. Cryst. Liq. Cryst.* **284**, 211 (1996).
- ³³E. Demiralp and W. A. Goddard III, *J. Phys. Chem. A* **102**, 2466 (1998).
- ³⁴D. Pedron, R. Bozio, M. Meneghetti, and C. Pecile, *Phys. Rev. B* **49**, 10 893 (1994).
- ³⁵For a review, see D. Feinberg, S. Ciuchi, and F. de Pasquale, *Int. J. Mod. Phys. B* **4**, 1317 (1990).
- ³⁶For a metal the susceptibility $\chi(0)$ can be approximated by the density of electronic states per monomer at the Fermi level, calculated, for example, by Y.-N. Xu, W. Y. Ching, Y. C. Jean, and Y. Lou, *Phys. Rev. B* **52**, 12 946 (1995).